Monte Carlo series analysis of irreversible self-avoiding walks. I. The indefinitely-growing self-avoiding walk (IGSAW)

1985 J. Phys. A: Math. Gen. 18 1515

(http://iopscience.iop.org/0305-4470/18/9/031)

J. Phys. A: Math. Gen. 18 (1985) 1515-1531. Printed in Great Britain

Monte Carlo series analysis of irreversible self-avoiding walks. I: the indefinitely-growing self-avoiding walk (IGSAW)

K Kremer† and J W Lyklema

Institut für Festkörperforschung der Kernforschungsanlage Jülich, D-5170 Jülich, Postfach 1913, Federal Republic of Germany

Received 31 August 1984, in final form 21 December 1984

Abstract. High-precision Monte Carlo data are used to estimate the exponents which govern the asymptotic behaviour of the recently introduced indefinitely-growing self-avoiding walk in two dimensions. For this walk the exponent γ is by definition equal to one. Applying the same methods which are used to extract the exponents from exact series enumeration, we give an estimate for the exponent ν of 0.567 ± 0.003. The leading corrections to this asymptotic behaviour are also calculated.

1. Introduction

Recently a new self-avoiding walk has been introduced (Kremer and Lyklema 1985) which is both completely self-avoiding and truly kinetic. This means that although the walk grows for ever, no site can be visited more than once. Thus we can look at this walk as a self-avoiding walk with the special property that it grows indefinitely (truly kinetic) or alternatively as a random walk with the additional constraint that it can occupy a particular site only one time (self-avoiding). This so called indefinitely-growing self-avoiding walk (IGSAW) is constructed in such a way that it recognises and avoids cages, no matter how large, which terminate the walk. Recently other irreversible SAW have been introduced but none of them possess both of the above described properties. The true SAW (TSAW, Amit *et al* 1983) is a truly kinetic model but is not self-avoiding, whereas the growing self-avoiding walk (GSAW, Hemmer and Hemmer 1984, Majid *et al* 1984, Lyklema and Kremer 1984a, b) is self-avoiding, but is not truly kinetic because it can get trapped. Notice that all the above mentioned walks are irreversible except the usual SAW. This irreversibility shows up in the one-step transition probabilities, e.g. these probabilities can differ if we look along the chain in the two different directions.

In this paper we present a detailed analysis of high-precision Monte Carlo data for IGSAW on a square lattice up to a length of $N = 100$ steps. To study the asymptotic behaviour of the mean square end-to-end distance $\langle R^2(N)\rangle$ and the next higher moment $\langle R^4(N)\rangle$ we apply the same techniques as we have previously used in the exact-enumeration study of this walk. In addition we have also calculated the mean square radius of gyration $\langle R_G^2(N)\rangle$ and the next moment $\langle R_G^4(N)\rangle$. The leading asymptotic

† Address until 30 August 1985: Exxon Research, Annandale, NJ 08801, USA; address thereafter: Institut für Physik, Johannes-Gutenberg-Universität Mainz, D-6500 Mainz, Postfach 3980, FRG.

behaviour of these quantities is described by a power law with an exponent ν:

$$\langle R^2(N)\rangle \propto \langle R_G^2(N)\rangle \propto N^{2\nu}. \tag{1}$$

Because of the high accuracy of our data it is also possible to study the corrections to scaling. In this way we have extended our earlier exact-enumeration analysis ($N_{max} = 22$) using the Monte Carlo technique to a regime where the assumption of the asymptotic behaviour of $\langle R^2(N)\rangle$ is much more reliable. Also from $\langle R_G^2(N)\rangle$ we can now expect to obtain an accurate result.

The paper is organised as follows. In the next section we give a definition of the IGSAW and explain the basic properties of the model in more detail than in the preceding letter (Kremer and Lyklema 1985). In § 3 we explain the Monte Carlo simulation, in particular the decision procedures for the construction of the walk. The numerical results are given in § 4 and the conclusions and a summary in § 5.

2. The IGSAW: the model and its basic properties

To define the IGSAW we have to give the one-step transition probabilities which completely describe the walk. We describe the construction procedure of the walk on the square lattice. The extension to other two-dimensional lattices is straightforward and will be briefly explained later on (see also figure 3(b)). At step one we have to choose between $q_0 = 4$ directions, in which case the one-step probability p_1 equals $1/q_0$. For the next step we have trivially $p_2 = 1/q = 1/(q_0 - 1)$ as for the usual SAW, which is in fact defined by this transition probability for all steps. The SAW is then terminated if it tries to violate the self-avoiding condition.

To define the transition probability for the IGSAW we first count how many of the nearest-neighbour sites have not been visited before. Let $n_i \leq q$ be this number at step i. So far we only have a local knowledge about the surroundings. This is clearly not enough to prevent the walker from entering cages which cause termination at some later step. In order to avoid such cages we need additional global knowledge of the conformational structure of the chain. This information is given by the winding number W_i at step i

$$W_i = \sum_{j=1}^{i} w_j. \tag{2}$$

This number is the sum over all angles w_j where j runs over all preceding steps. The w_j are counted as -1 for a clockwise angle of 90° between step j and step $(j-1)$, $+1$ for a counterclockwise angle and 0 when the walk proceeds straight ahead (w_0 and w_1 are equal to zero). For different two-dimensional lattices we obviously need a slight modification of this definition. This winding number W_i defines what is 'inside' and 'outside' when a cage can be entered. To find out if a cage is present we have to check if one of the nearest neighbours or one of the next-nearest neighbours, which form a half circle as drawn in figure 1(a) (encircled sites), has already been visited. If this were the case, the walk would consequently enter a cage; to avoid this, the site is disregarded as a possible jump site. The number of jump sites is at least one but less than or equal to n_i. The one-step transition probability can thus be defined as

$$p_i = 1/\text{number of jump sites}. \tag{3}$$

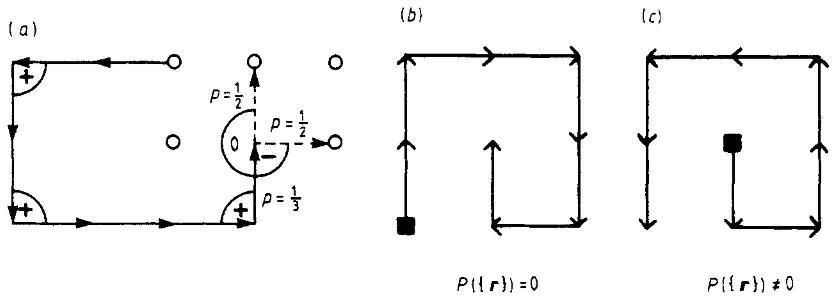

Figure 1. (*a*) A simple example of a short IGSAW, which already displays the property of avoiding cages. (*b*) This configuration does not fulfil the IGSAW conditions and therefore $P(\{r\}) = 0$; (*c*) this walk is a short IGSAW with $P(\{r'\}) \neq 0$. These simple configurations show the importance of irreversibility.

With this definition the IGSAW is completely defined. The jump sites are defined in such a way that the self-avoiding condition is fulfilled and no termination can occur. This can be done because the winding number W_i contains the relevant history of the walk and always recognises what is 'outside' for a particular configuration. Note that this information comes from the local analysis of the surroundings of the end of the walk. From this description it should be clear that a similar procedure for a three-dimensional lattice is much more complicated and unfortunately a practical method has not yet been found.

A typical example of an IGSAW is shown in figure 2. This computer-generated walk of length $N = 100$ builds large cages, suggesting a considerable excluded volume effect. Also the irreversibility can be seen from this figure, namely in those points where the

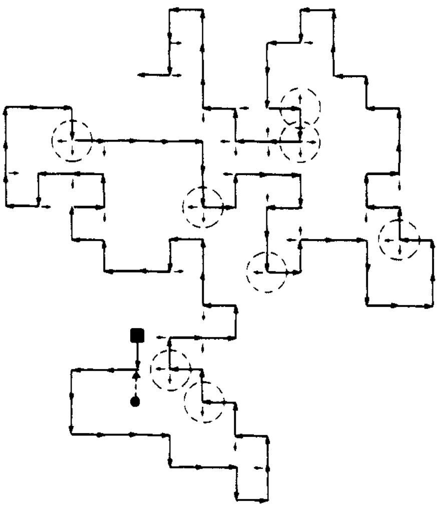

Figure 2. Typical example of a computer generated IGSAW of length $N = 100$. The dashed circles give the positions where the winding number analysis is relevant for the survival of the walk. If the first bond were to be the dotted one (---●), which would change the probability of the whole walk by a factor of 3/2, the inverse direction would no longer be an IGSAW and would therefore be forbidden (see also figure 1(*b*)).

chain touches itself. The open circles in this figure denote the sites where the walk could have travelled into a cage. At these positions the winding number defines the outward direction as one can easily check by performing the sum in equation (2) as given in figure 2. For the IGSAW the irreversibility, which is shown in figure 2, is a much stronger constraint than for the GSAW (Hemmer and Hemmer 1984, Majid *et al* 1984, Lyklema and Kremer 1984a, b). For $d=2$ the GSAW loses its irreversibility on the honeycomb lattice (Klein 1984). This cannot occur for the IGSAW. Figures 1(*b*) and 1(*c*) show the most simple examples which illustrate this and also define the 'active' end of the walk. Figure 1(*c*) shows an IGSAW configuration with probability $P(\{\boldsymbol{r}\})=\frac{1}{4}(\frac{1}{3})^4(\frac{1}{2})^2$ while the configuration in figure 1(*b*) is not an IGSAW and therefore $P\equiv 0$. For $d=2$ it is always possible for $N\to\infty$ to find the origin of the walk. More precisely, as soon as the end site N and a previous site $i\geqslant 0$ build a cage, which includes site number 0 in its interior, the inverse configuration is not an IGSAW and is therefore forbidden. The probability that this occurs very rapidly approaches 1 with increasing N.

From this information, the behaviour of the partition function $Z(N)$ can easily be deduced (Kremer and Lyklema 1985). Using the one-step probabilities of equation (3) the probability $P(\{r\}_N)$ of a configuration $\{r\}_N$ of a N-step IGSAW is simply $P(\{\boldsymbol{r}\})=\Pi_{i=1}^{N} p_i$. Because the walker never stops, which means that conservation of probability holds, one gets for the partition function

$$Z(N)=\sum_{\{r_N\}} P(\{r_N\})\equiv 1. \tag{4}$$

With the usual expression (for SAW), $Z(N)\propto(q_{\text{eff}}/q_0)^N N^{\gamma-1}$ (de Gennes 1979) the fixed point is equal to one (equation (6)) and

$$\gamma=1. \tag{5}$$

This gives for the generation function $G(x)$

$$G(x)=\sum_N Z(N)x^N \overset{x\to x_c^+}{\propto} (x-x_c)^{-\gamma}. \tag{6}$$

Because $Z(N)\equiv 1$ one directly finds $x_c=1$ and $\gamma=1$ (equation (5)). So far this is the only known analytical result for this walk. It shows that this model is a truly kinetic SAW. For a discussion of the partition function of such kinetic systems see, for example, Nakanishi and Family (1984) and Stella *et al* (1984). Before turning to the Monte Carlo procedure, we briefly want to explain a few other properties of the IGSAW. In comparison with the usual SAW we see that the possible configurations of the IGSAW form a subset of those of the SAW (Kremer and Lyklema 1985). Obviously all the SAW trajectories which cannot form part of an infinitely long chain are excluded configurations. As the asymptotic behaviour of the walks is given by the infinite trajectories, at a first glance it could be expected that both walks have the same asymptotic exponent ν. However, the IGSAW always finds its way out of dense situations and according to equation (3) such configurations have a higher probability than more expanded ones. Taking this into account it is clear that, as found from the exact enumeration (Kremer and Lyklema 1985)

$$\langle R^2(N)\rangle_{\text{SAW}} > \langle R^2(N)\rangle_{\text{IGSAW}}. \tag{7}$$

3. The Monte Carlo procedure

The chains are generated by the well known static-sampling procedure (see, for example, Kremer *et al* (1982) and references therein). For each new step the possible new directions are first selected. Then the new step $(i+1)$ is taken from these directions at random. On the square lattice there is a choice of at least one and at most three possibilities. These possibilities are calculated as follows. First the three nearest-neighbour sites are checked to see if one has been visited before. Secondly it must be determined whether one of the free sites leads into a cage. To find out if such a cage can be formed in the next step, the two next-nearest-neighbour sites in the forward direction must also be checked to see if they have been visited before (see figure 1). If one of these sites or the nearest-neighbour site in between them is occupied already at the kth step we have to calculate the difference winding number ΔW

$$\Delta W = W_i - W_k. \tag{8}$$

If ΔW is positive no step in a counterclockwise loop is allowed and, vice versa, no step in a clockwise loop is allowed when ΔW is negative. The possibility $\Delta W = 0$ does not occur because a cage can then not exist. In figure 3 we have illustrated the above discussion with some examples including simple examples for the honeycomb and the triangular lattice. Figure 4 again explains the algorithm for a configuration containing

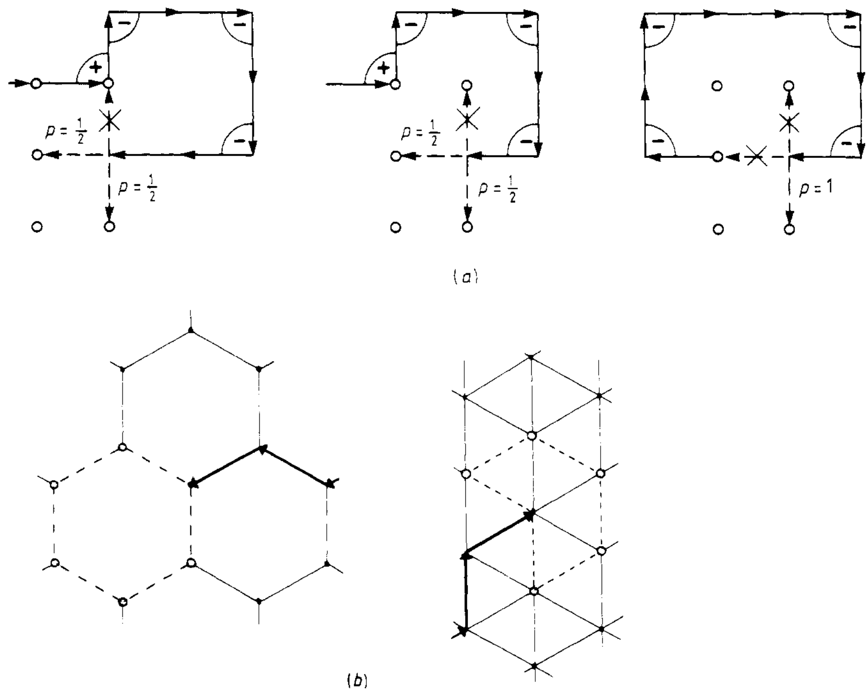

Figure 3. (*a*) The typical topological situations which occur during the walk construction. The encircled lattice sites give the positions which have to be analysed for the square lattice. Note that for the IGSAW two of these sites are next-nearest neighbours. (*b*) The relevant sites are encircled for the construction of an IGSAW on a honeycomb lattice and on the triangular lattice. Note that for the triangular lattice additional winding variables must be introduced to the ± 1 and 0 of the square lattice.

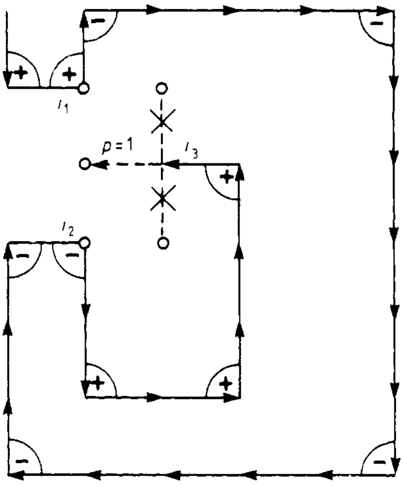

Figure 4. Example of a configuration which displays the most complicated topology which can occur. This part of the walk consists of two nested loops with opposite winding directions. The encircled sites again give the relevant sites for the construction algorithm. The difference in the winding number of step i_3 and i_1 ($\omega_{i_3}-\omega_{i_1}=-2$) defines 'outward' by proceeding straight forward or by turning through a +90° angle. The difference between step i_2 and i_1 ($\omega_{i_3}-\omega_{i_2}=\mp 2$) (the inner loop) defines 'outward' by proceeding straight forward or by turning through a −90° angle. Both restrictions then allow the walk to go only straight ahead.

nested loops. Such configurations are topologically the most complicated ones which can occur. To provide a different perspective on the above description, we study oriented curves in two dimensions. Non-crossing closed lines always enclose an angle of $\pm 2\pi$. The sign of the angle and the orientation of the last bond define the inside and outside of the loop. On the square lattice we measure the angles in units of $\pi/2$. The algorithm thus has to check whether a step to a non-occupied (NN) site can build a loop via a NN contact *and* whethei this new step points into this loop. This is given by the orientation of the last bond and the difference of the winding numbers at the contact points. If it points inside, the step is forbidden; otherwise it is allowed. In this way we have generated up to 4×10^7 chains of length $N=100$.

From these configurations we have then calculated the mean square end-to-end distance

$$\langle R^2(N)\rangle = \langle(\boldsymbol{r}_N-\boldsymbol{r}_0)^2\rangle \tag{9}$$

and the fourth moment

$$\langle R^4(N)\rangle = \langle(R^2(N))^2\rangle. \tag{10}$$

Here $\boldsymbol{r}_N$ and $\boldsymbol{r}_0$ are the positions of the Nth monomer and the zeroth monomer respectively. We have also calculated the mean square radius of gyration and its fourth moment for even values of N only (to save computer time)

$$\langle R_G^2(N)\rangle = \frac{1}{N+1}\sum_{i=0}^{N}\langle(\boldsymbol{r}_i-\boldsymbol{r}_{CM})^2\rangle \tag{11}$$

$$\langle R_G^4(N)\rangle = \langle(R_G^2(N))^2\rangle \tag{12}$$

with

$$\boldsymbol{r}_{\mathrm{CM}}=\frac{1}{N+1}\sum_{i=0}^{N}\boldsymbol{r}_i. \tag{13}$$

In addition we have calculated the mean displacement $\langle(\boldsymbol{r}_N-\boldsymbol{r}_0)\rangle$ in order to check the quality of the data. Ideally this quantity should be zero. Using this deviation we have typically found a discrepancy of 0.01% in $\langle R^2(N)\rangle^{1/2}$, showing the high accuracy of the data. The calculations have been performed on an IBM 3081 in extended precision (real *16). The calculation took about 30 h to complete—roughly the same amount of time we took for the exact enumeration ($N\leqslant 22$, Kremer and Lyklema 1985). In this latter calculation we have not included the very time-consuming radius of gyration calculation. Thus the advantage of a Monte Carlo calculation comes from the possibility of simulating much longer chains for which one can also calculate $\langle R_{\mathrm{G}}^2(N)\rangle$. Combining our exact enumeration results and the high-precision Monte Carlo data enables us to give an accurate estimate of the asymptotic behaviour of $\langle R^2(N)\rangle$ and $\langle R_{\mathrm{G}}^2(N)\rangle$.

4. Extrapolation methods and results

To extract results from our data we have used two standard methods from series analysis (see, for example, Djordjevic *et al* 1983). There exist of course more sophisticated methods like a Padé analysis, but data of much higher accuracy are then required (Pearce 1978). Also there seems to be no need to go beyond simple ratio methods because our results are as good as one can expect from Monte Carlo data.

To analyse our data we assume the following asymptotic behaviour for the mean square end-to-end distance and the mean square radius of gyration (for a more general discussion of corrections to scaling see, for example, Privman 1984):

$$\langle R^2(N)\rangle = A_R N^{2\nu}(1+B_R N^{-\Delta_R}+C_R N^{-1}+\ldots) \tag{14}$$

$$\langle R_{\mathrm{G}}^2(N)\rangle = A_{\mathrm{G}} N^{2\nu}(1+B_{\mathrm{G}} N^{-\Delta_{\mathrm{G}}}+C_{\mathrm{G}} N^{-1}+\ldots). \tag{15}$$

In these expressions ν is the critical exponent we are looking for. In brackets, the possible leading corrections to scaling are described by a correction term proportional to $N^{-\Delta}$ and an analytical correction proportional to N^{-1}. An important question to be settled before one can give a reliable estimate for ν is whether Δ is larger than one. This can be seen from the expressions for the effective exponents $\nu(N)$ which are defined in the two methods A and B as follows:

$$\begin{aligned}\nu_i^{\mathrm{A}}(N) &\equiv \frac{N}{2i}\left(\frac{\langle R^2(N+i)\rangle}{\langle R^2(N)\rangle}-1\right)\\ &= \nu-\tfrac{1}{2}\Delta B N^{-\Delta}-\tfrac{1}{2}CN^{-1}+\tfrac{1}{2}i\nu(2\nu-1)N^{-1}+\ldots\end{aligned} \tag{16}$$

and

$$\begin{aligned}\nu_i^{\mathrm{B}}(N) &\equiv \frac{1}{2}\,\frac{\ln(\langle R^2(N+i)\rangle/\langle R^2(N)\rangle)}{\ln[(N+i)/N]}\\ &= \nu-\tfrac{1}{2}\Delta B N^{-\Delta}-\tfrac{1}{2}CN^{-1}+\ldots.\end{aligned} \tag{17}$$

From these expressions we can estimate ν by plotting the calculated $\nu(N)$ against

$1/N$. This asymptotically results in a straight line if $\Delta > 1$. Only then can we extrapolate $\nu(N)$ to get a reliable estimate for ν. In this way we have analysed $\langle R^2(N)\rangle$ and $\langle R^4(N)\rangle$ for $i = 1, 2$ and 4 and $\langle R_G^2(N)\rangle$ and $\langle R_G^4(N)\rangle$ for $i = 2$ and 4. In figure 5 the results obtained from $\langle R^2(N)\rangle$ are plotted for method B and $i = 2$ and 4. Equation (17) already shows the advantages of method B. Here the corrections which describe the behaviour of $\nu^{B}(N)$ clearly have a simpler structure than for method A. This is also of importance for estimating the corrections to the leading behaviour. The data for $\nu(N)$ already show a linear behaviour with $1/N$ for N larger than 16, indicating that the assumption $\Delta > 1$ is correct. This supports our previous results from exact enumerations (Kremer and Lyklema 1985) and gives a first estimate of $\nu = 0.567$.

To analyse this in more detail we have studied the difference

$$\begin{aligned} D(N) &= \nu_2^{B}(N) - \nu_2^{B}(N-2) \\ &= \Delta^2 B N^{-(1+\Delta)} + C N^{-2}. \end{aligned} \tag{18}$$

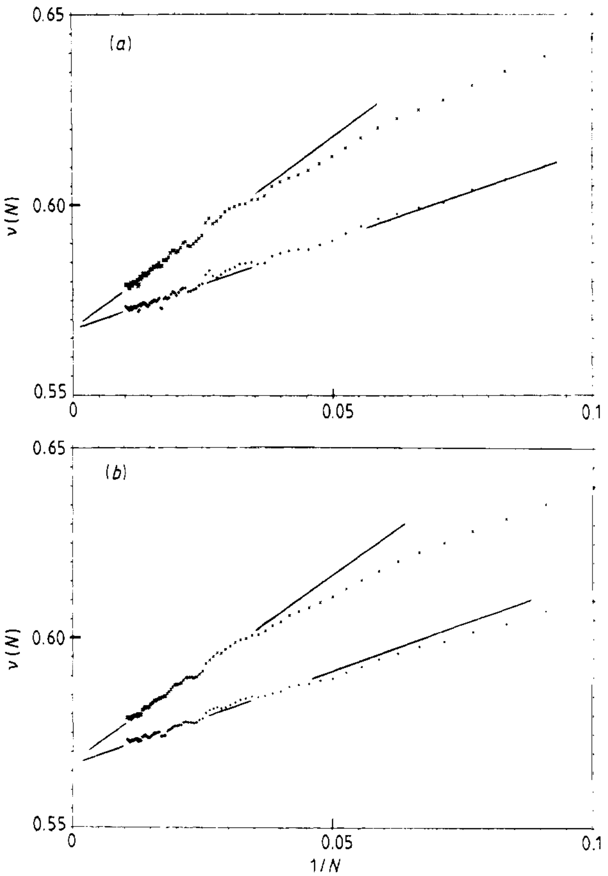

Figure 5. Plot of $\nu(N)$ using equation (17) for $\langle R^2(N)\rangle$ (lower curve) and using the analogous expression for $\langle R^4(N)\rangle$ (upper curve) against $1/N$ for $98 \geq N \geq 10$ and (a) $i = 2$ and (b) $i = 4$. Note that for $N \leq 20$ no distinction can be made between the MC data and the enumeration results. In order to have a realistic impression of the errors *no* averaging over various data points has been made.

This result is obtained by substituting equation (17) into the left-hand side of equation (18). The analysis of $D(N)$ versus N^{-2} for the enumeration data clearly shows a tendency to linear behaviour for $N \geq 14$. Note that for this analysis it is not necessary to know the value of ν. The data for $D(N)N^2$ and $\ln(D(N))/\ln N$ are given in table 1. There we also present the raw MC and enumeration data. From the enumeration data we conclude that asymptotically $D(N)$ is given by

$$D(N) \propto 1.05\ N^{-2}. \tag{19}$$

Table 1. Results for $D(N) = \nu(N) - \nu(N-2)$ from the enumerations for $\nu(N)$ calculated using equation (18).

N	$\frac{1}{2}\ln(D(N))/\ln N$	$D(N)N^2$
12	1.015	0.927
14	1.003	0.984
16	0.999	1.004
18	0.997	1.016
20	0.996	1.027

This estimate is nicely consistent with the same analysis of the Monte Carlo data. They are, of course not precise enough to improve the accuracy of equation (19). For this an accuracy of at least one order of magnitude higher would be needed for the MC results. Using this information equation (17) can be rewritten as

$$\nu(N) = \nu + \tfrac{1}{2}(1.05\ N^{-1}). \tag{20}$$

We estimate from the enumeration data for ν the value 0.57. Because this analysis is based on a rather short series ($N \leq 22$) of which only the last three points suggest an asymptotic behaviour it is highly desirable to study much longer series. This can only be done using a Monte Carlo technique and combining both results. After the foregoing discussion it is not surprising to see that the Monte Carlo data in figure 5 can be fitted very well by a straight line. For small N the fit is nearly perfect. For larger N the scatter increases because it becomes more and more difficult to sample all the walks adequately due to the tremendous number of possibilities. For large N we have sampled up to 4×10^7 walks which gives an accuracy of better than 0.02% for the mean square displacement (see also table 2). Estimated from the scatter in the data this still results in an error of 0.5% per point for such a sensitive quantity as a critical exponent. However, due to the large number of points it is possible to give an accurate estimate from a two-parameter least-squares fit for ν and C assuming linear behaviour with $1/N$. The values we have found are

$$\begin{aligned} \nu &= 0.567 \pm 0.003 \\ C &= -1.00 \pm 0.10. \end{aligned} \tag{21}$$

The value of C is checked by fitting $\nu = \nu(N) + \frac{1}{2}C/N$ to a zero-slope line in figure 6. Note that C is the only fit parameter in this plot. It should be mentioned that C, the correction to scaling amplitude, obtained by the MC data is in good agreement with the enumeration value (equation (19), $C = -1.05$). The errors here are estimated from the results obtained by fitting a varying number of points from subintervals of different

Table 2. Enumeration results for $N \leqslant 22$ for the IGSAW on the square lattice. N gives the number of steps, while Conf gives the number of different configurations. The partition function $Z(N)$ is always equal to 1. $\langle R^2 \rangle$ and $\langle R^4 \rangle$ are calculated using equations (9) and (10).

N	Conf	$Z(N)$	$\langle R^2 \rangle$	$\langle R^4 \rangle$	$\langle R^6 \rangle$
2	3	0.100 000 00E+01	0.266 666 67E+01	0.800 000 00E+01	0.266 666 67E+02
3	9	0.100 000 00E+01	0.455 555 56E+01	0.258 888 89E+02	0.164 555 56E+03
4	25	0.000 000 00E+01	0.674 074 07E+01	0.582 222 22E+02	0.579 851 85E+03
5	71	0.100 000 00E+01	0.900 000 00E+01	0.107 864 20E+03	0.151 122 22E+04
6	195	0.100 000 00E+01	0.114 279 84E+02	0.177 358 02E+03	0.326 625 51E+04
7	541	0.100 000 00E+01	0.138 779 15E+02	0.268 358 02E+03	0.621 242 94E+04
8	1 475	0.100 000 00E+01	0.164 508 46E+02	0.382 738 00E+03	0.107 730 96E+05
9	4 041	0.100 000 00E+01	0.190 343 70E+02	0.521 606 16E+03	0.174 176 62E+05
10	10 965	0.100 000 00E+01	0.217 056 47E+02	0.686 376 24E+03	0.266 614 95E+05
11	29 811	0.100 000 00E+01	0.243 887 75E+02	0.877 943 70E+03	0.390 570 96E+05
12	80 589	0.100 000 00E+01	0.271 383 80E+02	0.109 741 77E+04	0.551 955 76E+05
13	218 021	0.100 000 00E+01	0.298 991 67E+02	0.134 554 41E+04	0.756 990 70E+05
14	587 635	0.100 000 00E+01	0.327 147 88E+02	0.162 325 82E+04	0.101 223 25E+06
15	1 584 243	0.100 000 00E+01	0.355 397 45E+02	0.193 118 00E+04	0.132 450 36E+06
16	4 259 937	0.100 000 00E+01	0.384 119 38E+02	0.227 012 79E+04	0.170 092 36E+06
17	11 454 841	0.100 000 00E+01	0.412 926 72E+02	0.264 064 72E+04	0.214 884 88E+06
18	30 742 703	0.100 000 00E+01	0.442 144 68E+02	0.304 345 11E+04	0.267 589 86E+06
19	82 498 935	0.100 000 00E+01	0.471 444 73E+02	0.347 903 92E+04	0.328 991 05E+06
20	221 065 461	0.100 000 00E+01	0.501 108 50E+02	0.394 804 69E+04	0.399 895 89E+06
21	592 272 339	0.100 000 00E+01	0.530 850 16E+02	0.445 093 03E+04	0.481 131 85E+06
22	1584 987 143	0.100 000 00E+01	0.560 919 46E+02	0.498 827 01E+04	0.573 548 37E+06

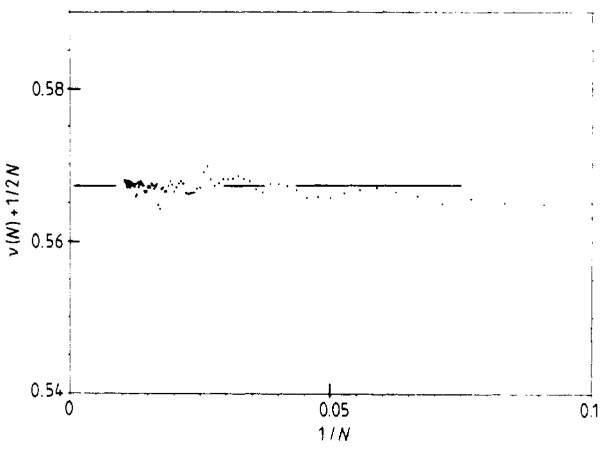

Figure 6. Plot of $\nu(N)+\frac{1}{2}CN^{-1}$ against $1/N$. $\nu(N)$ is determined from $\langle R^2(N)\rangle$ and $i=2$ using equation (17). This plot is the most sensitive check for determining C, the amplitude of the leading correction to scaling. The data give $C = 1.00 \pm 0.10$ in excellent agreement with the earlier enumeration results. Note the strongly enhanced scale for $\nu+\frac{1}{2}CN^{-1}$ compared to figure 5.

lengths. Here we have analysed $\nu_2^{\mathrm{B}}(N)$ only, but the same results are obtained if we study $\nu_i^{\mathrm{B}}(N)$ for $i \neq 2$, $\nu_i^{\mathrm{A}}(N)$ or if we study the fourth moments as can be seen from the figures. For the radius of gyration the situation is more complicated. As already can be seen from its definition (equations (11) and (13)) the mean square radius of gyration $\langle R_G^2(N)\rangle$ for a fixed value of N is governed by much smaller internal distances than the corresponding distance from $\langle R^2(N)\rangle$. From this, one can expect that the asymptotic behaviour for $\langle R_G^2(N)\rangle$ will occur for larger N values (see also table 3). Also the values of the correction terms are not necessarily the same. To study this we have again analysed $\nu_2^B(N)$ and plotted it against $1/N$ now for R_G^2. This gives a very smooth curve which extrapolates to a value of $\sim$0.573 for ν, which is not consistent with the result from $\langle R^2(N)\rangle$. However, the data do not seem to lie on a straight line;

Table 3. MC results for $10 \leqslant N \leqslant 100$. The column headed 'walks' gives the number of walks which are sampled. $\langle R^2\rangle$ and $\langle R^4\rangle$ are again calculated using equations (9) and (10) while $\langle R_G^2\rangle$ and $\langle R_G^4\rangle$ are given by equations (11)–(13). Note that for $\langle R_G^2\rangle$ and $\langle R_G^4\rangle$ a smaller number of walks is sampled.

N	Walks	$\langle R^2\rangle$	$\langle R^4\rangle$	Walks	$\langle R_G^2\rangle$	$\langle R_G^4\rangle$
10	7 360 000	21.6899	685.4719	1150 000	3.4009	12.945 6
11	7 360 000	24.3725	876.8932			
12	7 360 000	27.1244	1 096.2213	1150 000	4.2503	20.3886
13	7 360 000	29.8852	1 344.0491			
14	7 360 000	32.7036	1 621.8046	1150 000	5.1320	29.9288
15	7 360 000	35.5251	1 929.2320			
16	7 360 000	38.3942	2 267.6759	1150 000	6.040 5	41.7032
17	7 360 000	41.275 3	2 638.1196			
18	7 360 000	44.1995	3 040.9494	1150 000	6.971 6	55.8239
19	7 360 000	47.1315	3 476.5542			
20	7 360 000	50.0984	3 956.2170	1750 000	7.9228	72.3976
21	7 360 000	53.0681	4 447.3019			
22	7 360 000	56.0692	4 983.5579	1750 000	8.8906	91.5154
23	7 360 000	59.0779	5 554.5771			
24	7 360 000	62.1152	6 160.7440	1750 000	9.8752	113.2791
25	7 360 000	65.1697	6 803.5813			
26	7 360 000	68.2468	7 482.7275	1750 000	10.8751	137.7760
27	7 360 000	71.3375	8 199.5117			
28	7 360 000	74.4475	8 952.7011	1750 000	11.8889	165.0808
29	7 360 000	77.5573	9 740.4986			
30	7 360 000	80.7026	10 569.6473	2390 000	12.9158	195.2535
31	7 360 000	83.8528	11 435.6710			
32	7 360 000	87.0304	12 341.7653	2390 000	13.9543	228.3783
33	7 360 000	90.2124	13 287.7069			
34	7 360 000	93.4143	14 273.5492	2390 000	15.0038	264.5176
35	7 360 000	96.6224	15 299.9590			
36	7 360 000	99.8500	16 265.8726	239 .000	16.0636	303.7029
37	7 360 000	103.0775	17 471.0965			
38	7 360 000	106.3260	18 616.9040	2390 000	17.1336	346.0218
39	7 360 000	109.5862	19 803.8816			
40	16 500 000	112.8784	21 040.9220	3080 000	18.2155	391.6194
41	16 500 000	116.1535	22 308.9588			
42	16 500 000	119.4457	23 618.6796	3080 000	19.3043	440.3992
43	16 500 000	122.7408	24 969.5525			
44	16 500 000	126.0484	26 362.5979	3080 000	20.4018	492.4802
45	16 500 000	129.3633	27 797.3539			
46	16 500 000	132.6894	29 274.6927	3080 000	21.5068	547.8797
47	16 500 000	136.0258	30 798.2856			

Table 3. (continued)

N	Walks	$\langle R^2\rangle$	$\langle R^4\rangle$	Walks	$\langle R_G^2\rangle$	$\langle R_G^4\rangle$
48	16 500 000	139.3855	32 370.6911	3080 000	22.6192	606.6520
49	16 500 000	142.7449	33 982.7739			
50	16 500 000	146.1201	35 638.4737	3780 000	23.7390	668.9171
51	16 500 000	149.4925	37 335.8932			
52	16 500 000	152.8794	39 080.4534	3780 000	24.8654	734.5599
53	16 500 000	156.2803	40 872 6664			
54	16 500 000	159.6901	42 709.3020	3780 000	25.9988	803.7291
55	16 500 000	163.1020	44 589.9722			
56	16 500 000	166 5203	46 512.4003	3780 000	27.1384	876.4345
57	16 500 000	169.9482	48 481.0749			
58	16 500 000	173.3893	50 497.8741	3780000	28.2844	952.7276
59	16 500 000	176.8306	52 560.5694			
60	27 300 000	180.2567	54 659.9988	4630 000	29.4390	1032.7669
61	27 300 000	183.7196	56 817.7527			
62	27 300 000	187.1935	59 019.4392	4630 000	30.5973	1116.3464
63	27 300 000	190.6677	61 267.6593			
64	27 300 000	194.1529	63 562.3700	4630 000	31.7616	1203.6513
65	27 300 000	197.6481	65 908.6043			
66	27 300 000	201.1506	68 299.3869	4630 000	32.9317	1294.6915
67	27 300 000	204.6536	70 737.4001			
68	27 300 000	208.1734	73 228.0447	4630 000	34.1070	1389.4713
69	27 300 000	211.6888	75 761.3580			
70	27 300 000	215.2158	78 344.1712	5620 000	35.2886	1488.1840
71	27 300 000	218.7428	80 973.5680			
72	27 300 000	222.2857	83 651.3542	5620 000	36.4741	1590.5924
73	27 300 000	225.8344	86 380.2515			
74	27 300 000	229.3924	89 159.9508	5620 000	37.6645	1696.8603
75	27 300 000	232.9577	91 992.4273			
76	27 300 000	236.5311	94 871.8744	5620 000	38.8598	1807.0182
77	27 300 000	240.1038	97 796.4868			
78	27 300 000	243.6858	100 771.7922	5620 000	40.0598	1921.1034
79	27 300 000	247.2790	103 805.0564			
80	40 500 000	250.8533	106 861.3683	6830 000	41.2618	2038.8756
81	40 500 000	254.4559	109 990.8819			
82	40 500 000	258.0618	113 168.1877	6830 000	42.4710	2160.9328
83	40 500 000	261.6728	116 393.9414			
84	40 500 000	265.2936	119 673.8022	6830 000	43.6849	2287.0405
85	40 500 000	268.8159	123 001.5471			
86	40 500 000	272.5500	126 384.1045	6830 000	44.9035	2417.2362
87	405 00 000	276.1869	129 820.5543			
88	40 500 000	279.8284	133 304.8293	6830 000	46.1263	2551.5286
89	40 500 000	283.4721	13 837.3381			
90	40 500 000	287.1304	140 430.9064	8420 000	47.3503	2689.5755
91	40 500 000	290.7905	144 074.6794			
92	40 500 000	294.4546	147 764.5360	8420 000	48.5809	2832.0498
93	40 500 000	298.1200	151 505.0363			
94	40 500 000	301.7974	155 304.8957	8420 000	49.8153	2978.6699
95	40 500 000	305.4788	159 159.6228			
96	40 500 000	309.1676	163 068.0948	8420 000	51.0535	3129.4629
97	40 500 000	312.8621	167 031.2396			
98	40 500 000	316.5622	171 045.6748	8420 000	52.2955	3284.4527
99	40 500 000	320.2693	175 119.9084			
100	40 500 000	323.9847	179 241.2046	8420 000	53.5414	3443.6847

they still show a slightly increasing curvature. There may be two reasons for this; either the data are not yet in the asymptotic region or the leading correction to scaling is not proportional to $1/N$. To analyse this in more detail we rewrite equation (17) for $\langle R_G^2(N)\rangle$ as

$$\ln(\nu_2^B(N)-\nu_{est}) = \ln(-\tfrac{1}{2}\Delta_G B_G) - \Delta_G \ln N. \tag{22}$$

Here we have assumed that for the radius of gyration we have $\Delta_G < 1$ and $B_G < 0$, an assumption which is suggested by the N dependence of the data. For ν_{est} we take the value 0.567 from the $\langle R^2(N)\rangle$ analysis. A plot of equation (22) is given in figure 7. From the resulting straight line we estimate

$$\Delta_G = 0.64 \pm 0.10. \tag{23}$$

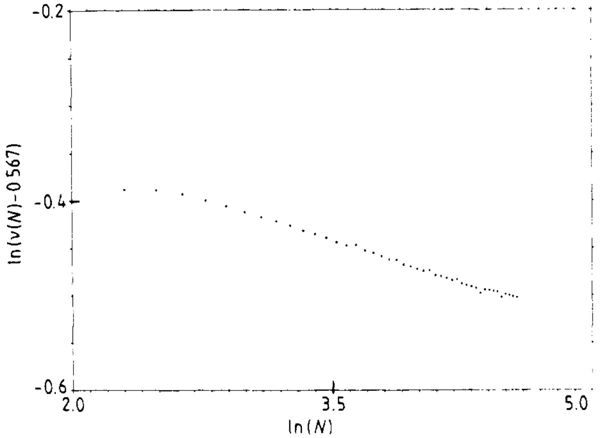

Figure 7. Plot of $\ln(\nu(N)-\nu_{est})$ against $\ln N$ using equation (22) for $\langle R_G^2\rangle$ and $i=2$ to determine the leading correction to scaling. For ν_{est} we took the asymptotic ν value as deduced from the $\langle R^2(N)\rangle$ data, $\nu = 0.567$. The data nicely fit a straight line with a slope which gives $\Delta = 0.64$. Note that the scatter of the data determines the errors especially for the data at $N = 90, 80, 70\ldots$ because there $\nu(N)$ connects statistically nearly-independent samples.

This is in remarkable contrast with the result for $\langle R^2(N)\rangle$ where we found $\Delta_R = 1$. To estimate ν from the radius of gyration data we have to plot $\nu_2^B(N)$ against $N^{-0.64}$ (see figure 8). This indeed results in a straight line for $N \geq 35$ which extrapolates to the expected value of 0.567. From the slope of this figure we then calculate

$$B_G = -0.92 \pm 0.10. \tag{24}$$

This value is confirmed by a one-parameter fit of $D(N)$ against $N^{-(1+\Delta)}$.

We now still have to calculate the prefactors A_R and A_G. With the above given values for the exponent and the correction terms we can estimate this from

$$A_R = \frac{\langle R^2(N)\rangle}{N^{2\nu}(1+C_R N^{-1})}$$
$$A_G = \frac{\langle R_G^2(N)\rangle}{N^2(1+B_G N^{-\Delta_G})}. \tag{25}$$

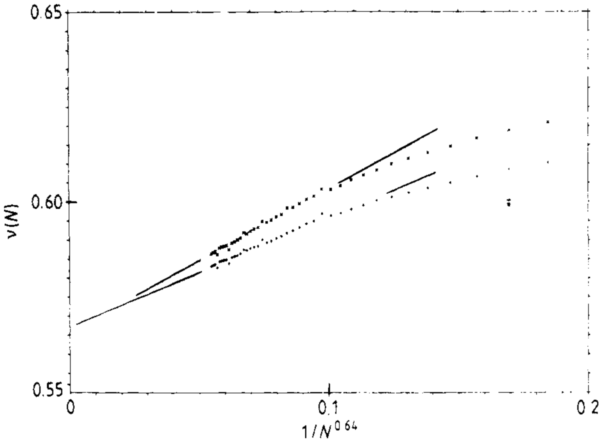

Figure 8. Plot of $\nu(N)$ against $1/N^{0.64}$ for $\langle R_G^2(N)\rangle$ (lower curve) and $\langle R_G^4(N)\rangle$ (upper curve) for $98 \geqslant N \geqslant 10$. $\nu(N)$ is calculated using equation (17) with $i=2$.

This results in

$$\begin{aligned} A_R &= 1.766 \\ A_G &= 0.303 \end{aligned} \tag{26}$$

and $\langle R_G^2(N)\rangle/\langle R^2(N)\rangle = A_G/A_R = 0.1652$ for $N=100$ where A_R, A_G and A_G/A_R still show a very small increase, which could change the last one or two digits a little. This amplitude ratio is surprisingly close to that of the usual random walk value of $\frac{1}{6}$, if not equal when the ratio is extrapolated to $N \to \infty$. Because we also have by construction $\gamma = 1$, this may suggest a very late asymptotic behaviour resulting also in a random walk value of $\frac{1}{2}$ for ν. However, our data are completely inconsistent with a logarithmic correction. This is illustrated in figure 9. Details are given in the figure caption. Also from the fact that for $N = 100$ the ratio is already practically $\frac{1}{6}$ whereas $\nu(N)$ does not show any sign of bending down to $\nu = \frac{1}{2}$, we conclude that we have assumed the correct asymptotic behaviour (equation (14)).

For the asymptotic ratios of the moments we find

$$\begin{aligned} &\langle R^2(N)\rangle/\langle R^4(N)\rangle^{1/2} = 0.77 \\ &\langle R_G^2(N)\rangle/\langle R_G^4(N)\rangle^{1/2} = 0.91. \end{aligned} \tag{27}$$

Thus we find for the asymptotic value of the variance

$$\begin{aligned} &\frac{(\langle R^4(N)\rangle - \langle R^2(N)\rangle^2)^{1/2}}{\langle R^2(N)\rangle} = 0.84 \\ &\frac{(\langle R_G^4(N)\rangle - \langle R_G^2(N)\rangle^2)^{1/2}}{\langle R_G^2(N)\rangle} = 0.45. \end{aligned} \tag{28}$$

This non-vanishing variance illustrates the need for high-precision calculations of these relatively short chains as opposed to much less accurate simulations for very long chains.

The last quantity which we have studied is the winding angle of the walk (Fisher *et al* 1984). We define $\theta(N)$ as the winding number in the units which we used for

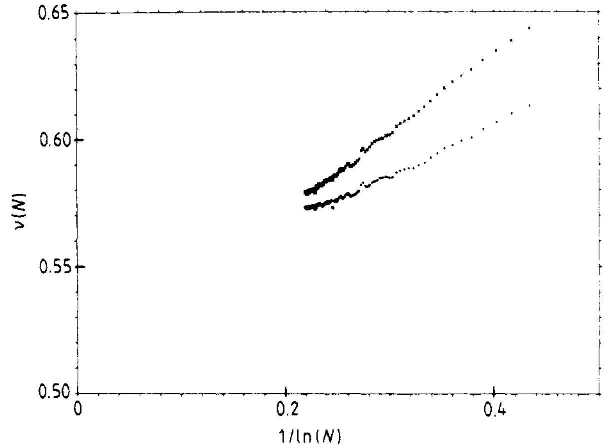

Figure 9. Plot of $\nu(N)$ against $1/\ln N$ for $\langle R^2(N)\rangle$ and $i=2$. Here $\nu(N)$ again is determined by equation (17). Assuming a behaviour of $\langle R^2(N)\rangle = AN^{2\nu}(\ln^{\alpha} N + \ldots)$, $\nu(N)$ should be proportional to $1/\ln N$. The data are clearly inconsistent with such an assumption. The main purpose of this figure is to test whether the data can bend down to $\nu = 1/2$ via a logarithmic correction. The slope of the data points in the opposite direction. In order to reach $\nu = 1/2$ the data must behave very strangely, with at least one inflection point.

the construction of the walk. For the asymptotic behaviour of $\langle \theta^2(N)\rangle$ we have assumed

$$\langle \theta^2(N)\rangle \sim (\ln N)^p. \tag{29}$$

From our analysis we find

$$p = 0.9 \pm 0.1. \tag{30}$$

This must be compared with 2.00 which one expects to hold for the RW and 1.22 which is found for the SAW. It is also argued, however, that this number should be one. We find the same behaviour for the ratio $\langle \theta^4(N)\rangle/\langle \theta^2(N)\rangle^2$. For the RW one expects to find the value 3. For the SAW the value approaches 3 from above, whereas for the IGSAW we always find that $\langle \theta^4(N)\rangle/\langle \theta^2(N)\rangle^2 < 3$ but increasing with N. A plot of $\langle \theta^4(N)\rangle/\langle \theta^2(N)\rangle^2$ against $1/N$ shows a distinct curvature even for $N = 100$. We estimate $3 \geqslant \langle \theta^4(N)\rangle/\langle \theta^2(N)\rangle^2 \geqslant 2.97$, but within the error bars the ratio can approach 3.

5. Conclusions

We have given a detailed analysis of the properties of the IGSAW, a truly kinetic *and* completely self-avoiding walk. By the use of high-precision Monte Carlo data we extended our previous series analysis of exact enumeration data ($N \leqslant 22$) (Kremer and Lyklema 1985) up to $N = 100$. Because of the high accuracy of the data (see the tables) we are able to apply the methods used in series analysis to analyse the data. Note that the plotted results are *never* smoothed by any kind of averaging over various points. Therefore the scatter of the data give a realistic estimate of the errors, without additional sources of errors which depend on how one analyses the data. The reason for simulating many, relatively short chains instead of sampling very long, but very few chains can be deduced from equation (28). The fluctuation of $\langle R^2\rangle$ and $\langle R_G^2\rangle$ show an asymptotically non-vanishing variance. For $\langle R^2(N)\rangle$ the variance stays at 0.84. This means that the width of the distribution function does not decrease! Therefore, to get data of high quality which is necessary for the calculation of critical exponents, a number of samples are needed which are, for N distinctly larger than 100, beyond the present computing possibilities. Therefore we claim that the present method is the best way to study such systems without spending an extraordinary amount of computing time. An additional check of the quality of the data is given by a comparison with the exact enumeration results (see the tables). They show a perfect coincidence, so that the two results in the foregoing figures are completely indistinguishable.

The corrections to scaling, as determined for $\langle R^2(N)\rangle$ and $\langle R_G^2(N)\rangle$, are much more difficult to determine. A first estimate for $\langle R^2(N)\rangle$ comes from the enumeration data. The leading N^{-1} correction to scaling for $\langle R^2(N)\rangle$ is excellently confirmed by the Monte Carlo results. Of course we cannot distinguish between $N^{-0.95}$ and $N^{-1.0}$ or a combination of such exponents, but we can conclude that the correction to scaling for $\langle R^2(N)\rangle$ is at least for one decade governed by an N^{-x} behaviour, with $x \simeq 1$. Because $\gamma = 1$ and also because amplitude ratios are the same as for random walks it could be argued that $\nu = 1/2$, and that there might be logarithmic corrections. In order to have such a situation, a very different result from what actually happens would be expected (see figure 9). In order to bend down to $\nu = 1/2$, figure 9 must have an inflection point, a highly unexpected feature. Our conclusion from the results for $\langle R^2\rangle$, $\langle R^4\rangle$, is that we can exclude such a behaviour and therefore our estimated error for $\nu = 0.567 \pm 0.003$ is reliable. A very interesting point is that the corrections to scaling for $\langle R_G^2\rangle$ are, within the chain length we analyse, proportional to $N^{-0.64}$ instead of N^{-1} as for $\langle R^2\rangle$. This is because $\langle R_G^2\rangle$ is governed by much smaller internal distances. $\langle R_G^2\rangle$ is defined as the mean square distance of all monomers from the centre of mass and can be rewritten (Flory 1969) as the average squared internal distance between all monomers. Taking this into account, at least a larger amplitude and possibly a smaller exponent for the corrections to scaling can be expected, compared to the ones for $\langle R^2\rangle$.

Because of the current controversy for the corrections to scaling for the usual SAW (see, for example, Privman 1984) it is very interesting to check these questions for these systems also (Lyklema and Kremer 1985). An open question is the extension of this model to three dimensions. It has been suggested by us (Kremer and Lyklema 1984) that this walk might have an upper critical dimension of three. Because of the non-triviality of this problem we have not yet studied this problem in three dimensions. Also for an analytical study of d_c which of course is highly desirable, it is first necessary to formulate the problem in three dimensions. The IGSAW is, compared with other kinetic growth models like diffusion-limited aggregation (Witten and Sander 1983), a more simple model. An analytical study of the present model might therefore give some insight in the difficulties encountered there. A physical realisation of this model could be the diffusion-limited growth of a chain on a surface. With the condition that the chain cannot relax during the growth process, this polymer should show up a typical IGSAW configuration.

Another question is whether there is any connection to the θ point of real polymers. This speculation came up in connection with the discussion of the GSAW (Majid *et al* 1984, Kremer and Lyklema 1985). However, there is still the question whether such irreversible kinetic models can describe equilibrium properties of physical systems. The other more striking arguments against a θ analogy is the behaviour discussed in figure 1(*b*), which for $N \to \infty$ always defines the origin of the walk, in strong contrast with the θ point behaviour of a polymer where there is no preferred end. Also this walk may describe the cluster-hull properties (Weinrib and Trugman 1984). Although the numerical results for ν given here are in very good agreement with numerical results for the cluster hull (Voss 1984) the same arguments concerning the 'origin' of the walk for the θ discussion again show that the IGSAW is topologically different from the cluster hull. The cluster hull can be described by a modified IGSAW, which grows symmetrically and therefore does not have any distinguished origin. For a ring closing version Weinrib and Trugman (1984) showed this for clusters on the triangular lattice.

To summarise we have presented an extensive numerical analysis of the recently introduced indefinitely-growing self-avoiding walk IGSAW (Kremer and Lyklema 1985). The exponent γ is equal to 1. For the exponent ν we find from $\langle R^2\rangle$, $\langle R^4\rangle$, $\langle R_G^2\rangle$ and $\langle R_G^4\rangle$ extrapolations $\nu = 0.567 \pm 0.003$. The leading correction to scaling is proportional to N^{-1} for $\langle R^2\rangle$ while it is proportional to $N^{-0.64}$ for $\langle R_G^2\rangle$:

$$\begin{aligned} R^2(N) &= 1.77\ N^{2\times 0.567}(1 - 1.00\ N^{-1} + \ldots) \\ R_G^2(N) &= 0.30\ N^{2\times 0.567}(1 - 0.92\ N^{-0.64} + \ldots). \end{aligned} \tag{31}$$

Besides these exponent the corresponding amplitudes and amplitude ratios are determined, including the winding angle ratios.

References

Amit D J, Parisi G and Peliti L 1983 *Phys. Rev.* B **27** 1635

Djordjevic Z V, Majid J, Stanley H E and dos Santos R J 1983 *J. Phys. A: Math. Gen.* **16** L519

Fisher M E, Privman V and Redner S 1984 *J. Phys. A: Math. Gen.* **17** L569

Flory P J 1969 *Statistical Mechanics of Chain Molecules* (New York: Interscience)

de Gennes P G 1979 *Scaling Concepts in Polymer Physics* (Ithaca, NY: Cornell UP)

Hemmer S and Hemmer P C 1984 *J. Chem. Phys.* **81** 584

Klein D J 1984 private communication

Kremer K, Baumgärtner A and Binder K 1982 *J. Phys. A: Math. Gen.* **15** 2879

Kremer K and Lyklema J W 1985 *Phys. Rev. Lett.* **54** 267

Lyklema J W and Kremer K 1984a *J. Phys. A: Math. Gen.* **17** L691

—— 1984b *Proc. Int. Topical Conf. on Kinetics of Aggregation and Gelation* (*University of Georgia, Athens, USA*) *1984* (Amsterdam: North-Holland)

—— 1985 *Phys. Rev.* B **31** 3182

Majid J, Jan N, Coniglio A and Stanley H E 1984 *Phys. Rev. Lett.* **52** 1257

Nakanishi H and Family F 1984 *J. Phys. A: Math. Gen.* **17** 427

Pearce C J 1978 *Adv. Phys.* **27** 89

Privman V 1984 *Physica* A **123** 428

Stella A L, de Queiroz S L A, Duxbury P M and Stinchcombe R B 1984 *J. Phys. A: Math. Gen.* **17** 1903

Voss R F 1984 *J. Phys. A: Math. Gen.* **17** L373

Weinrib A and Trugman S 1985 *Phys. Rev.* B **31** 2993

Witten T A and Sander L M 1983 *Phys. Rev.* B **27** 5686